Ferromagnetic resonance in nanostructures, rediscovering its roots in paramagnetic resonance.

Klaus Baberschke†

Institut für Experimentalphysik, Freie Universität Berlin, Arnimallee 14, D-14195 Berlin, Germany

Abstract. Both techniques went different routes: The EPR explored an enormous variety of paramagnets in solids, liquids, and gas phase. The focus was to determine orbital- and spin-magnetic moments (g-tensor), hyperfine interactions, and from the linewidth the spin dynamics (T_1, T_2 relaxation). In FMR most of the experiments and theory assumed the total value M to be constant in the equation of motion and used only one effective damping parameter (Gilbert). This is an enormous, unnecessary limitation for today's analysis of magnetism in nanostructures and ultrathin films. To assume M = const ignores spin wave excitations, scattering between longitudinal and transverse components of M. Moreover, in the framework of itinerant ferromagnetism, the magnetic moment/atom μ was assumed to be isotropic with $g \approx 2$! That ignores the anisotropy of μ in nanostructures and the importance of the orbital magnetic moments with $\mu_L/\mu_S = (g-2)/2$. Without finite μ_L we would have no magnetic anisotropy energy (MAE), no hard magnets, no magnetic storage media. Only recently the "language" of EPR was adapted to FMR in ultrathin films. A g-tensor is discussed and its interrelation with the MAE is pointed out. Also recent theory points out, that "*there is no reason to assume a fixed magnetization length for nanoelements*". This allows a detailed discussion of magnon-magnon scattering, spin-spin, and spin-lattice relaxation - useful, for example, for fs spin dynamics. Recent FMR experiments using frequencies from 1 GHz up to several hundred GHz, will allow measuring the proper g-factor components and μ_L, μ_S. From the frequency dependent linewidth magnon-magnon scattering can be separated from dissipative spin-lattice damping.

Version: 5 August 2011

PACS numbers: 75.75.+a,76.50.+g,76.30.-v

1. Historical reminiscences

Shortly after the discovery of EPR, here in Kazan, Altshuler and Kosyrew published a comprehensive book. Immediately after, this book was translated into German [1], it is one of the first EPR-textbooks, others appeared more recently (e.g.[2]). The main focus of EPR experiments with transition metal ions in solid state physics was to determine orbital- and spin- magnetic moments, the chemical bonding of the magnetic ion, its coupling to the nuclei, and its spin dynamic. In Fig.1 this is visualized in short, illustrating the difference of the development in the ferromagnetic resonance (FMR), as reviewed in the next paragraph. Low symmetry and spin-orbit coupling (SOC) splits the e_g and t_{2g} degeneracy and mixes excited states into the ground state. In

† E-mail: bab@physik.fu-berlin.de, http://www.physik.fu-berlin.de/∼bab

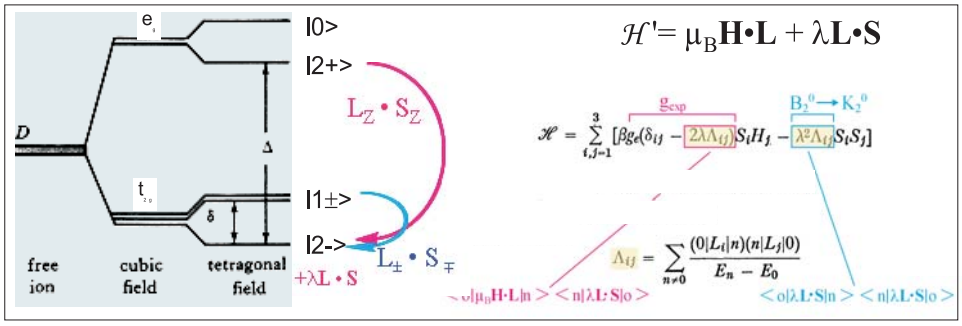

Figure 1. Schematic sketch of d-level energy splitting, the SOC, and the perturbative part of the Spin Hamiltonian $\mathcal{H}'$. For details see text and [1, 2].

second order perturbation theory the Λ_{ij} matrix elements enter and modify the energy levels and EPR spectrum in to ways: They modify the magnetic moment of the ion, the g-factor components, and they produce an additional energy splitting, the so-called *zero field splitting* (ZFS), the D or B_2 parameters. This is textbook knowledge and was tabulated and did characterize numerous paramagnetic crystals and solids. Important for EPR and FMR students is, that Fig.1 visualizes the same origin for anisotropic magnetic moments and the ZFS, namely the admixture of excited states into the ground state by SOC. As an exercise for students it is interesting to note that the off diagonal part of the SOC mixes also different spin states (orientations), "−" goes to "+" and vice versa.

The FMR went a complete different route. The resonant microwave absorption in ferromagnetic metals for a given frequency, let's say X-band, is controlled by an effective field $H_{\rm eff}$ (see Fig.2), which is a vector sum of an external applied field and various contributions of internal magnetization. Consequently it is almost impossible to disentangle the product of the torque term in the Landau-Lifshitz equation (LL) (Fig.2). In addition, a larger fraction of the literature, treats $3d$ ferromagnets (FM), like Fe and Co, in the framework of *itinerant ferromagnets* with delocalized d-band electrons with an isotropic value of $g \approx 2$. Very little is said about an anisotropic

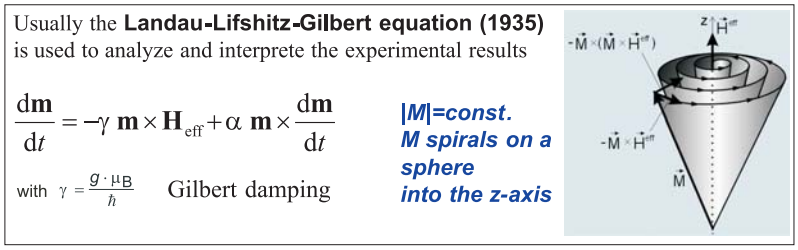

Figure 2. Standard equation of motion for a constant magnetization M in an external field.

magnetic moment per ion, for example in Fe, Co, Ni in the standard literature of the *fundamentals of nanomagnetism* [3, 4]. However, this is important for a proper Hamiltonian $\mathcal{H}'$ (Fig.1). An isotropic γ or g value, as given in the LL-equation (Fig.2), ignores this. For example, the magnetic moment μ per atom in Ni single crystals is larger along the [111] direction (see Fig.3 and [5]). Clearly the effect is small ($< 10^{-3}$)

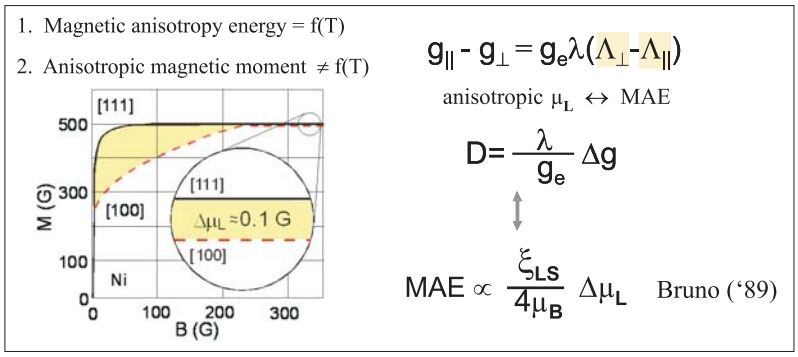

Figure 3. Magnetic Anisotropy Energy (MAE) and orbital magnetic moment μ_L and its interrelation via 2^{nd} order perturbation theory. For details see [5].

but all important. Otherwise we would not understand hard and easy axis in FM. We will come back to this in Section 2.

Fig.2 illustrates another handicap or "incompleteness" in frequently reasoning of the spin-dynamics in FM nanostructures [4]: It is assumed that the length of the magnetization vector M is constant. If so, than it is clear that with some constant α, the Gilbert damping in the LLG equation, the vector spirals on a sphere into the z-axis. This is energy dissipation, an irreversible process. In the early days of magnetism this may have been justified, experiments were carried out at ambient temperature or below and the Curie temperatures were at $T_C \approx 1000$ or 1300 K. A

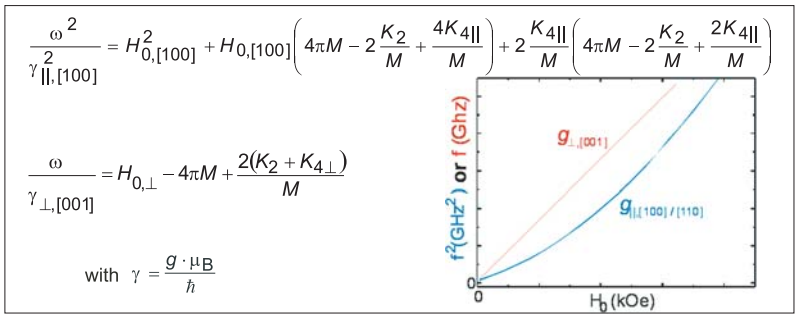

Figure 4. FMR resonance equation for in-plane and out-of plane orientation of the external field H_0 with respect to the crystallographic film plane. For details and notation, see[6, 7].

$T = 0$ approach was reasonable, but for ultrathin films and nanostructures with low T_C, this ignores important information, which is contained in the FMR linewidth. Not to be misunderstood, there exists classical literature discussing spin-wave excitations at finite temperatures and more than one relaxation channel, e.g. Harry Suhl in [8] and the nice book about *Magnetic Oscillations and Waves* [9]. But this literature is cited and used very little by the FMR community. The majority of FMR papers, review article, and textbooks use as an equation of motion the LLG equation (Fig.2) with **one relaxation channel**, only. This is an unnecessary limitation, it ignores spin-wave excitation at finite T. Historically it may be understandable, because in the early days there was a heavy debate whether spin-waves could exist in ferromagnetic metals.

One opinion (Peter Wohlfarth, et al.) said, no spin waves only Stoner excitations are important in metallic FM. Others, like David Edwards, could show that long lived spin waves indeed exist in metals. In Sec.3 we show how magnon-magnon scattering can be extracted from the FMR linewidth [7, 10].

2. Orbital- and spin-magnetic moments μ_L, μ_S in ferromagnetic monolayers

Is it possible to measure the g-tensor components and energy splitting (ZFS or MAE) in magnetic resonance experiments separately? If yes, this will be a great success, because both parameters are related, as indicated in Fig.1 and Fig.3. In Fig.4 the solution of the LL-equation is given for two orientations of the external field (for a more general solution, see [7]). For in-plane orientation we have a quadratic dependence of $\omega(H)$, and a linear dependence for out-of-plane. But in both cases there are internal contributions to the local field [6]. These contributions make it very difficult to determine γ or g on the left hand side of the equation, if only **one** frequency is used. Consequently most publications in FMR of metallic FM assume $g \approx 2$ or keep $g =$ const and determine only the MAE and K_i parameters in the analysis of angular dependent FMR experiments. In Sec.1 and Fig.1 we mentioned the interrelation between ZFS, D, B_2 and the Δg. This is a standard knowledge for EPR. In Fig.3 we show the corresponding case for FMR: MAE $\propto \Delta\mu_L$ and the EPR Bleaney parameters $\mathbf{B}_n^m$ can be related to the MAE parameters $\mathbf{K}_n^m$ in FMR. Surprisingly, this standard treatment (Fig.1) in EPR was transfered to itinerant electrons in the language of band structure and k-space very late, only in 1989 by Patric Bruno (Fig.3) [11]. With this pioneering work one bridge was established between localized and itinerant pictures of EPR and FMR in metals.

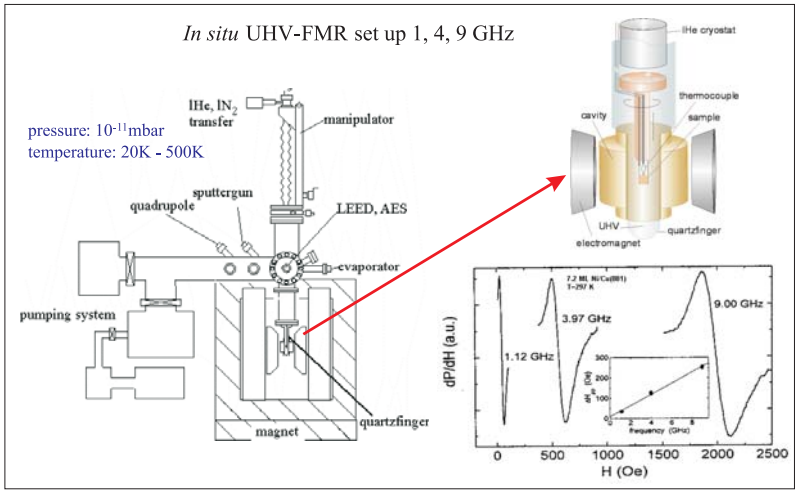

Figure 5. EPR, FMR spectrometer in combination with an UHV-chamber. The sample is prepared and characterized with LEED, AES, etc in the upper level. The long manipulator moves the specimen down into the quarzfinger and rotates it with respect to H_0 [12, 13].

If however, multifrequency FMR is used, the first term at the right hand side of the resonance equation in Fig.4 depends only on the external field, H_0, which is know very

precisely. Today multifrequency EPR and FMR is no problem, commercial equipment for low frequencies 1, 4, 9 GHz is available, as well as frequency analyzer and high frequencies up to THz. This allows to measure in addition to the K_i parameters also γ or g, as indicated in a sketch of Fig.4. This new development of GHz technology makes the full potential of the FMR technique accessible.

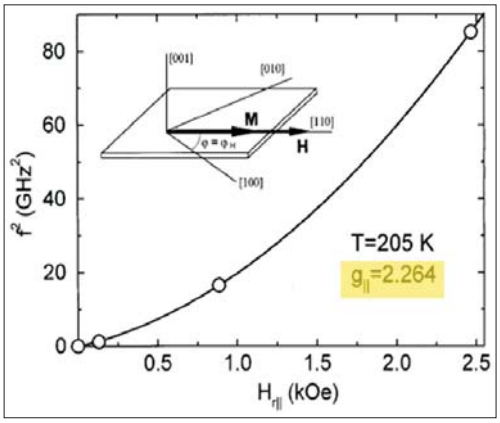

Figure 6. Analysis of $g_{\|}$ for Fe_2V_5 according to the equation given in Fig.4.[14].

In Fig.5 a set-up of an UHV-FMR spectrometer is shown. In the bottom part of the UHV chamber a quartzfinger is mounted with an one inch diameter. This allows very easily to replace standard cavities with "large excess hole" of 9, 4, 1 GHz (Varian, Bruker). One example is given for 7 ML of Ni on a Cu single crystal surface (inset, Fig.5). The ultrathin film stays in perfect UHV, no protecting cap layer is needed. The microwave cavity operates in normal laboratory air. Within 30 min. cavity and frequency can be changed and the identical sample is measured at different microwave frequencies. Note the narrow linewidth at 1 GHz, the frequency dependent plot of $\Delta H(\omega)$ ends for $\omega = 0$ almost at zero on the y-axis, no apparent residual linewidth at $\omega = 0$ appears [3]. Details of the set-up, its sensitivity, the preparation of ultrathin films, and the adsorption of molecules, are given in [7, 12, 13].

In Fig.6 and 7 FMR results for a Fe_2V_5 multilayer or a Fe_2/V_5 superlattice is shown[14]. The data follow perfectly a parabola of $f^2(H_r)$ with one g-factor component of $g_{\|} = 2.26$. Note, that the spectroscopic g-factor is a fundamental proportionality factor for the magnetic moment μ. In some FMR literature g is used as a simple fitting parameter, yielding different values for 9 and 24 GHz, for example. Other publications report on temperature dependent g-factors at low T. This should not be mixed up with the discussion of orbital- and spin-magnetic moments, as defined in EPR. It indicates only the difficulties to extract proper g-values in FMR. The table in Fig.7 (top right) and diagram (bottom left) show the results. From the g-factor for Fe_2V_5 we determine an orbital moment of 13 % for μ_L/μ_S. This is 3 to 4 times larger than in bulk Fe. The diagram also shows the change of the μ_L/μ_S ratio for thicker Fe_4 superlattice films and for bulk Fe. Another experimental technique, the X-ray Magnetic Circular Dichroism (XMCD), also measures orbital- and spin-moments, by applying the sum rules (for details of XMCD see [15].) The right-hand diagram in Fig.7 shows the element selective XMCD results, measured at the $L_{3,2}$ absorption edges of V and Fe. This is of interest, because it tells us, that at interfaces of FM films

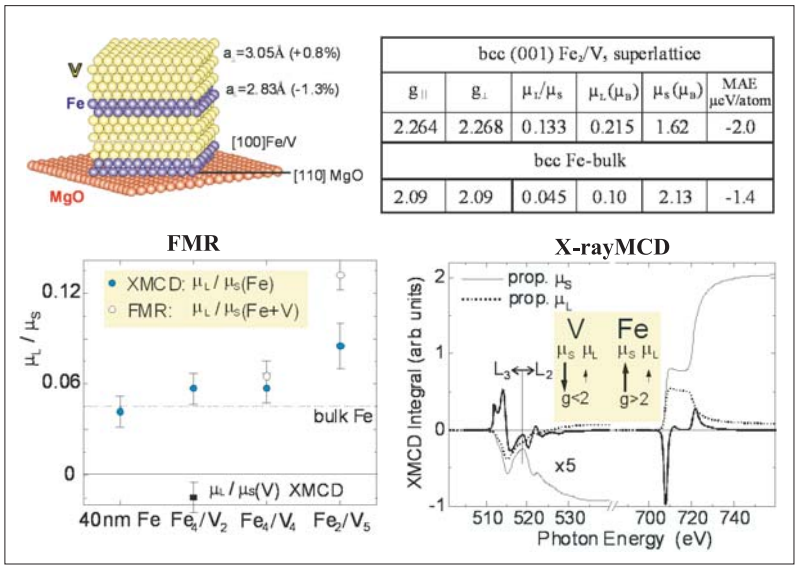

bcc (001) Fe_2/V, superlattice					
$g_{\parallel}$	$g_{\perp}$	μ_L/μ_S	$\mu_L(\mu_B)$	$\mu_S(\mu_B)$	MAE μeV/atom
2.264	2.268	0.133	0.215	1.62	-2.0
bcc Fe-bulk					
2.09	2.09	0.045	0.10	2.13	-1.4

Figure 7. Schematic sketch for epitaxial grown Fe_nV_m superlattice structure, FMR and XMCD results, table for g-factors, μ_L, and μ_S [7, 14].

and its nonmagnetic substrate or cap material, a magnetic moment may be induced at the nonmagnetic element. Here at the Fe/V interface a magnetic moment at V is induced with $\mu_L/\mu_S < 0$. This is in agreement with $g < 2$ for the beginning of the $3d$ series. For Fe it is opposite, $g > 2$. Therefore it is not a surprise, that the measured μ_L/μ_S value is larger in FMR than in XMCD. FMR is not element specific, it measures the total moment (Fe+V, see the arrows in the X-rayMCD Fig.). This result shows some warning, when discussing FMR results in nanostructures. An enhanced μ_L/μ_S ratio in FMR does not necesserily mean that μ_L is larger. On the other hand, FMR is in favor, it can measure both, the MAE and the g-tensor, as indicated in Sec.1 and Fig.3.

In summary: The handicap and misinterpretation in the past of FMR in nanostructures , was caused because only X-band (or at most K- and Q-band) were used [16]. Now with a multifrequency technique the full potential and a proper interpretation of FMR is available.

3. Spin-phonon, spin-spin dynamics

In Fig.8 two most popular equations of motion are given for the dynamics in magnetism. Most of the FMR community uses the LLG-equation, as discussed in Sec.1. In EPR and NMR very clearly a spin-spin and a spin-lattice relaxation rate are used. This can be formulated by the Bloch-Bloembergen (BB) equation. There exists some literature in which different relaxation channels in metallic FM are discussed [8, 9]. But the FMR community made very little use out of it. The resonant microwave absorption in a FM starts with a uniform motion of a $k = 0$ mode (Fig.8b), but this uniform mode can scatter into spin waves. In the cartoon of Fig.8 this is indicated by a variation of the transverse components of the magnetization. Path 2 in Fig.8b indicates this. It is in principle a reversible process, the energy stays in the magnetic

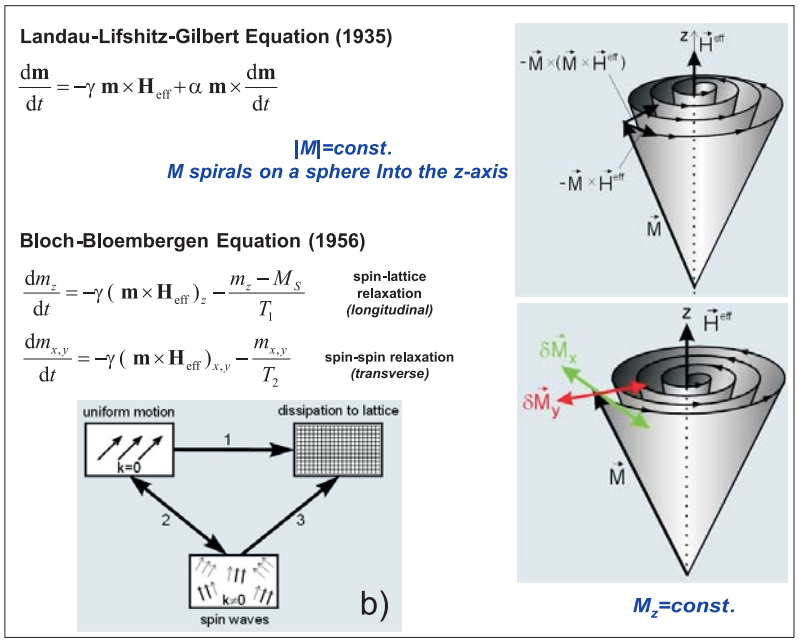

Figure 8. Two models for Larmor precision [1, 2, 9]. The arrows $\delta H_{x,y}$ indicate transverse spin scattering, dephasing, see text. Fig.8b is taken from [8].

subsystem. In contrast, path 1, a scatter to the lattice, is irreversible with energy dissipation [8]. Path 3 in Fig.8b indicates a magnon-phonon scattering. This is a vital research topic, currently, for femtosecond LASER pump-probe experiments. This community discusses very well transverse spin-spin relaxation, a T_2 process in the BB-model. Indeed, a *dephasing* in the spin wave dynamic is important. Details for metallic FM can be seen in [17].

So the question arises: Can FMR contribute to disentangle scattering within the magnetic subsystem from dissipation and energy flow to the thermal bath? The standard FMR literature uses the LLG equation and concludes *that the FMR linewidth is strictly linearly dependent on the microwave frequency* ω*...*[4] (left part of Fig.9). On the other hand, already Suhl stated that *spin wave excitations need to be taken into account...and...the LLG damping no longer apply....* Similar reasoning can be found in [9]. 1999 D. L. Mills and coauthors calculated magnon-magnon scattering in ultrathin films and its contribution to the FMR linewidth (right part of Fig.9)[18]. As they discuss: *Two magnon scattering is a dephasing event*, contributes to the transverse relaxation time T_2, but leaves the longitudinal relaxation time T_1 unaffected [19]. For such a process, which describes the time evolution of the total magnetization including magnon-magnon scattering, the LL equation is inappropriate. For ultrathin films, some given surface structure, and anisotropy, it appears that dipolar interaction between spins becomes important. As a consequence, the spin-wave dispersion relation is not anymore a parabola, but a superposition of linear and quadratic terms. This is indicated in the sketch $\omega(k)$ in Fig.9. Now it is easy to understand that the excitation of the uniform FMR mode is degenerated with a finite wave vector mode. These authors even, derive an analytical function for the contribution to the FMR linewidth due to magnon-magnon scattering, as given in Fig.9. Now we have two contributions

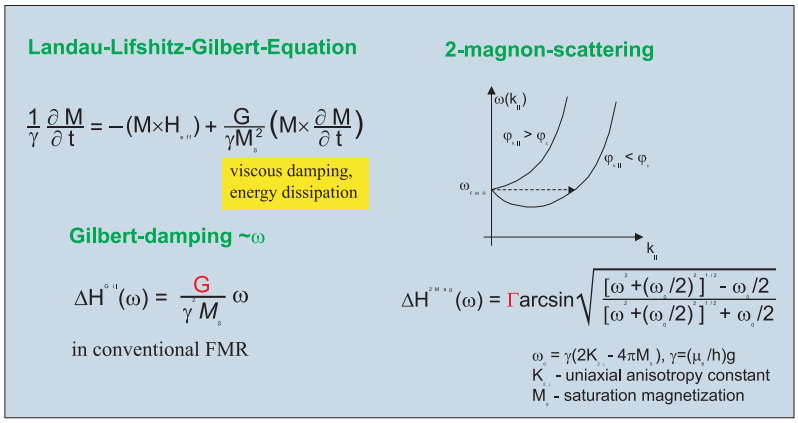

Figure 9. FMR linewidth in the LLG-model [3, 4] and for the 2-magnon-scattering [18, 19]. See text

to the FMR linewidth $\Delta H(\omega)$, the linear Gilbert damping with the prefactor G and an *arcsin* function for the 2-magnon scattering with prefactor Γ. All other parameters (M_S, K_2, ω_0) are known from the static resonance parameters.

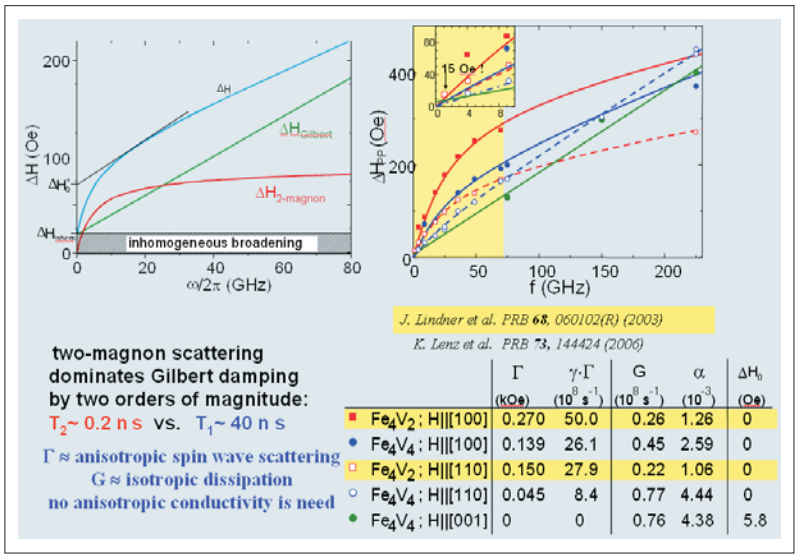

Figure 10. FMR linewidth of Fe_nV_m superlattices as function of microwave frequencies from 1 to 225 GHz. Left: as model; right: experimental results taken from [20, 21]. Note the very narrow ΔH for 1 GHz in the inset.

The left part of Fig.10 shows the result, a strong curvature at low frequencies and a saturation at high ω. In other words: For realistic parameters of ultrathin films magnon-magnon scattering strongly increases in the range of zero to 30 GHz, whereas the Gilbert damping increases slowly linear with the microwave excitation frequency. Here we demonstrate the importance of low frequency FMR. In former FMR analysis a residual linewidth ΔH_0 at $\omega = 0$ was discussed [3, 4]. This may be an erroneous

misinterpretation resulting from the fact, if only few frequencies (10, 24, 36 GHz) have been measured - one always can fit a linear line through two or three data points. If however at 1 GHz a very narrow linewidth is measured - like in Fig.5 and right-hand diagram of Fig.10 - it becomes evident that the measured ΔH is a relaxation and no inhomogeneous broadening! The data and diagram for Fe_4V_2 and Fe_4V_4 samples show clearly the two relaxation processes. For $H \perp$ to the film plane no magnon scattering is possible, consequently we see only a linear frequency dependence (green dots). For H in-plane strong magnon-magnon scattering is observed. Moreover, we observe that the Gilbert damping G is more or less isotropic for different orientations of H in the film plane, whereas the magnon-magnon $\gamma\Gamma$ is anisotropic by a factor of 2 or 3 for different in-plane orientation (Fig.10 Table) [19, 20, 21]. No residual linewidth was observed, the experimental width is purely a relaxation process. Finally, the fitting procedure yields numbers for the relaxation times. The spin-spin relaxation is about two orders of magnitude faster than the spin-lattice rate - a very plausible result. In the table of Fig.10 we give the Gilbert relaxation rates in dimensionless units of α and G in units of s^{-1}. The 2-magnon scattering rates/second are given as $\gamma\Gamma$ and as linewidth Γ in kOe. Field units (Oe) and dimensionless α parameters are very little informative. For a better understanding of fundamental resonance physics, we strongly recommend to return to the notation of EPR and give units of relaxation rates in s^{-1}. This is not a simple question of style and common language, it facilitates the communication with theory of femtosecond dynamics in magnetism.

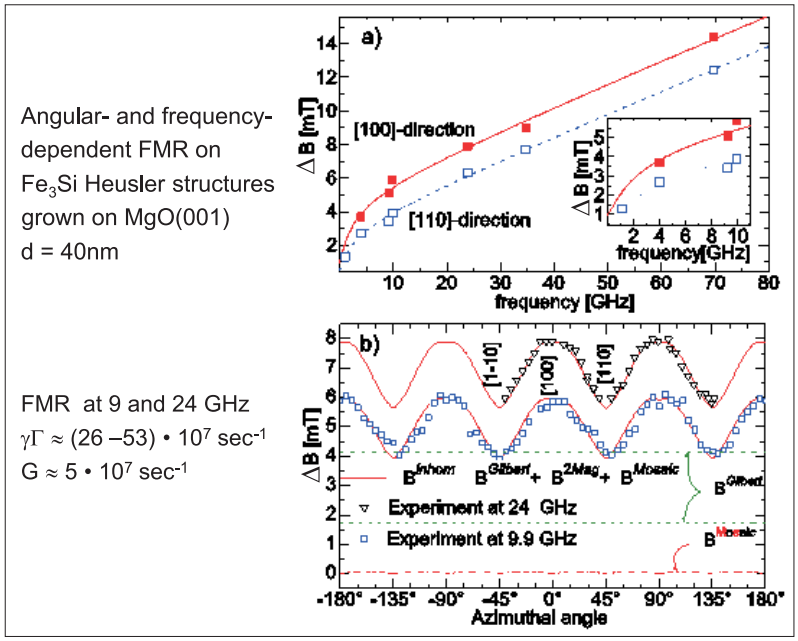

Figure 11. FMR linewidth for Heusler alloys as function of frequency taken from [23]. Note the narrow line at 1 GHz. Fig11b shows the angular dependent 2-magnon scattering and isotropic Gilbert damping.

The results in [20, 21] were the only experimental FMR measurement, which did check in a *quantitative way* the theoretical prediction for the magnon-magnon scattering [18, 19]. All the other FMR literature for more than 10 years from 1999

on, used only the LLG-equation [22]. Certainly the *arcsin* function may not be the ultimate solution, but experimentalists should proof or disproof existing models. Or even batter, they should not stick on old models, but publish experimental data free of bias.

Recently similar results have been observed for ultrathin Fe_3Si Heusler structures [23]. The film was grown epitaxially on a MgO single crystal surface. This is an interesting case because Heusler ultrathin films are used in many experiments of nanomagnetism, and if FMR can help to determine specific parameters for the spin dynamic, this will influence other interpretations of spin transport measurements. Fig.11 shows the result for the FMR linewidth measured from 1 to 70 GHz. Again, the non-linear frequency dependence of ΔB is seen, note the very narrow line at 1 GHz (inset of Fig.11a). More important is the frequency and angular dependent (azimuthal and polar) measurement. In Fig.11b the results are shown for two(!) frequencies, 9 and 24 GHz. With this complete set of FMR data the different contributions to the linewidth are separated: A strong angular dependent 2-magnon scattering with minimum along the [001] direction, an isotropic Gilbert damping, and a vanishing inhomogeneous line broadening was observed. The detailed analysis and fitting procedure by Zakeri et al. [23] used only the linewidth parameters for the fitting, all other input parameters have been determined before from the static resonance parameter (e. g. $g = 2.075$). As a results the authors find an isotropic Gilbert damping of $G \approx 5 \cdot 10^7$ sec^{-1}, a value which agrees very well with other Fe damping parameters. However the magnon-magnon scattering is not as fast as in the Fe/V superlattice, it is only a factor of 10 faster, than the Gilbert damping.

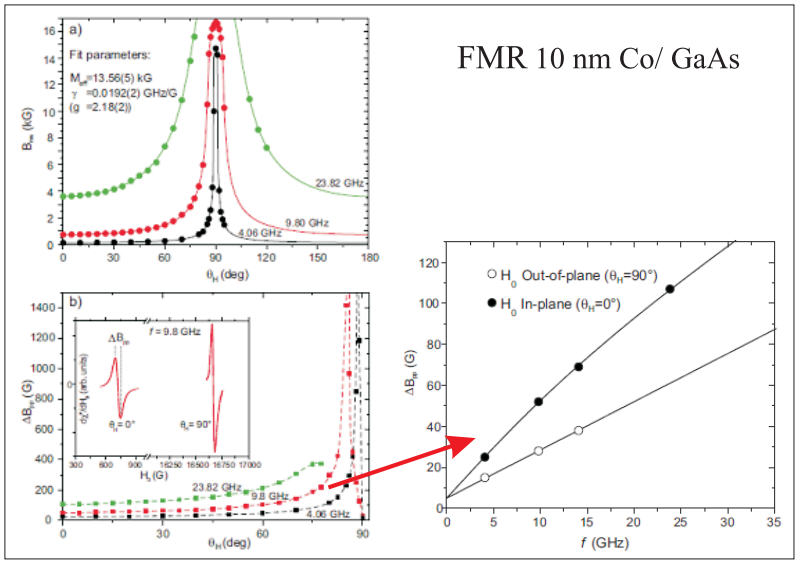

Figure 12. FMR resonance field and linewidth for a Co ultrathin film, measured at 4 frequencies, taken from [24].

For a long time the first experimental evidence for magnon-magnon scattering, determined from FMR has been ignored or criticized, to be a singularity and special feature of the Fe/V superlattice. The previous results at the Heusler structure gave some more confidence. As last and most recent case, we will shortly discus the FMR

experiments on pure Co films by Lindner et al. [24]. To measure the dynamical response of a prototype film of polycrystalline hcp Co film of about 10 nm thickness on GaAs is of general interest for spin dynamics in nanostructures. In Fig.12 the results are given. Fig.12a shows the field for resonance as function of the polar angle for 3(!) frequencies. As discussed in Sec.2, for a proper interpretation all data together need to be fitted with one set of parameters. As a result the g-factor of $g = 2.18$ is very close to bulk Co. The error bar of ± 0.02 is too large to see the anisotropy in hcp Co. With these numbers the frequency dependent linewidth (Fig.12b+c) can be fitted. The Gilbert damping of $G \approx 0.16 \cdot 10^9$ sec^{-1} is about a factor of 10 faster for polycrystalline specimen, than in high purity epitaxially grown films. The magnon-magnon scattering is in the same order of magnitude. The authors analyzed some residual linewidth at $\omega = 0$, however experiments at 1 GHz are missing. Our experience is, that in cases with 1 GHz FMR data the line narrows again, surprisingly. In other words: The remaining width may still be caused by scattering of some magnons in the range of few GHz.

So far we have discussed the LLG- and BB- model and the magnon-magnon scattering in the FMR linewidth by Arias and Mills [18]. This theory assumes a certain model structure on the surface of ultrathin FMs. Not to be misunderstood, this calculation and the classical models of spin dynamics are based on idealistic structures, which may be far from reality. More and better theory is needed for a better understanding of the FMR linewidth. But this is not the point. In Sec.3 we wanted to demonstrate the full potential of FMR linewidth analysis. Frequency dependent experiments will give the FMR the same full potential in linewidth analysis as it is a standard procedure in EPR.

4. Summary and future

Two aspects have been discussed for the future development of FMR in nanomagnetism: The static resonance conditions and the spin dynamics in the linewidth. The message of Sec.2 will be: The old-fashion standard procedure to discuss magnetism of 3d-metallic FM in the framework of e_g and t_{2g} levels with eigenstates like $d_{z^2}, d_{x^2-y^2}, d_{xy}, d_{xz}, d_{yz}$ is insufficient. It may explain some MOKE, STM, or photoemission experiments, but it misses orbital magnetism and MAE. For the above unperturbed 3d-eigenstates $\langle L_z \rangle = 0$. In reality the groundstate is an admixture via SOC with $\langle L_z \rangle \neq 0$, see Fig.1. This produces a g-tensor, to be measured by FMR, and an MAE, see Fig.4. The new development in multifrequency- and UHV-technology opens a huge field for FMR. Old-fashion experiments and review papers, for X-band only, etc. used the g-factor as a fitting parameter, but not as a fundamental property of the magnetic moment (different g values for X- and K-band were published).

The spin wave dynamics in magnetic nanostructures is a very active and broad research field, currently. Not only 2-magnon scattering, as discussed in Sec.3, is of interest. 4-magnon scattering, for example, has been discussed in a high condensate of magnons in YIG thin films. Microwave photons split into pairs of correlated magnons [25]. In the same material X-ray detected magnetic resonance was performed in the nonlinear regime of spin waves [26]. These authors discuss also the redistribution of energy within internal degrees of freedom of the spin system, before it is transferred to the lattice. They introduce also a T_1^{-1} and a T_2^{-1}, longitudinal and transverse, relaxation rates. In LASER pump-probe experiments [17] the authors discuss magnon induced damping and magnon-phonon scattering (path3 in Fig.8b). In particular these

experiments initiated new theories [27], the Landau-Lifshitz-Bloch equation (LLB). Two relaxation rates are introduced, $\alpha_\perp$ and $\alpha_\parallel$. Note, these rates are not identical to the phenomenological T_1^{-1} and T_2^{-1} rates in the BB model. Sec.3 demonstrates that todays FMR is able to measure separately scattering within the spin wave system and energy dissipation. Multifrequency experiments seem to be essential. This is possible, starting at ≈ 1 GHz up to THz [28].

Now, on the occasion of the 100^{th} anniversary of S. A. Altshuler it seems to be time that the young generation of FMR leaves the old-fashion path of LLG-equation, assuming an isotopic $g \approx 2$, fitting Gilbert parameter with an apparent linear frequency dependence. All this is not completely wrong, but it gives very little insight on the fundamental properties of nanomagnetism in 3d metallic FMs. Many of the more recent aspects in the interpretation of FMR of nanostructures, as discussed in Sec.2 and 3, are given in [29].

Acknowledgment

Intensive and ongoing discussions with D. L. Mills, M. Farle, J. Lindner, and K. Lenz are acknowledged. E. Kosubek and J. Kurde assisted in preparing this manuscript.

References

[1] S. A. Altshuler, B. M. Kosyrew *Paramagnetische Elektronenresonanz*, Teubner, Leipzig (1963)
[2] A. Abragam, B. Bleaney *Electron Paramagnetic Resonance of Transition Ions* W. Marshall, D. H. Wilkinson, Eds. Clarendon Press, Oxford, (1970)
[3] B. Heinrich and J. A. C. Bland, Eds.,*Ultrathin Magnetic Structures II*, Springer, Berlin (1994).
[4] J. A. C. Bland and B. Heinrich, Eds.,*Ultrathin Magnetic Structures III*, Springer, Berlin (2005).
[5] K. Baberschke, Lecture Notes in Physics, Springer **580**, 27 (2001)
[6] for a detailed discussion of K_2, K_4, etc., see M. Farle Rep. Prog. Phys. **61**, 755 (1998)
[7] K. Baberschke in H. Kronmüller and S. S. Parkin, Eds., *Handbook of Magnetism and Advanced Magnetic Materials* Vol. **3**, 1627 John Wiley & Sons, Ltd. (2007).
[8] Harry Suhl IEEE Transactions on Magnetics **34**, 1834 (1998)
[9] A. G. Gurevich and G. A. Melkov, *Magnetic Oscillations and Waves* CRC Press, Boca Raton, (1996).
[10] K. Baberschke Physica status solidi (b) **245**, 174 (2008)
[11] P. Bruno Phys. Rev. B **52**, 411 (1995)
[12] M. Zomack, K. Baberschke Surf. Sci. **178**, 618 (1986)
[13] J. Lindner and K. Baberschke J. Phys.: Condens. Matter **15**, R193 (2003)
[14] A.N. Anisimov, M. Farle, P. Poulopoulos, et al. Phys. Rev. Lett. **82**, 2390 (1999) and A. Scherz, H. Wende, P. Poulopoulos et al. Phys. Rev. B **64**, 180407 (2001)
[15] H. Wende Rep. Prog. Phys. **67**, 2105 (2004)
[16] In some FMR literature g-factors are fitted from angular dependent measurements at one frequency. This may lead to erroneous results. We believe only frequency dependent fits, as in Fig.6, will lead to unambiguous results.
[17] A. Melnikov et al. Phys. Rev. Lett. **100**, 247401 (2008) and U. Bovensiepen J. Phys. Condens. Matter **19**, 083201 (2007)
[18] R. Arias, D. L. Mills Phys. Rev. B **60**, 7395 (1999)
[19] D. L. Mills, S. M. Rezende in B. Hillebrands, K. Ounadjela (Eds.) *Spin Dynamics in Confined Magnetic Structures II*, Springer, Berlin (2003)
[20] J. Lindner, K. Lenz, E. Kosubek, K. Baberschke, et al. Phys. Rev. B **68**, 060102(R) (2003)
[21] K. Lenz, H. Wende, W. Kuch, K. Baberschke, et al. Phys. Rev. B **73**, 144424 (2006)
[22] Note that in [21] also earlier results by Woltersdorf and Heinrich have been reanalyzed.
[23] Kh. Zakeri, J. Lindner, I. Barsukov, R. Meckenstock, et al. Phys. Rev. B **76**, 104416 (2007) and Phys. Rev. B **80**, 059901 (2009)
[24] J. Lindner, I. Barsukov, C. Raeder, C. Hassel, et al. Phys. Rev. B **80**, 224421 (2009)
[25] S. O. Demokritov et al. Nature **443**, 430 (2006)
[26] J. Goulon et al. J. Mag. Mag. Mat. **322**, 2308 (2010)

[27] O. Chubykalo-Fesenko et al. Phys. Rev. B **74**, 094436 (2006) and D. A. Garanin et al. Phys. Rev. B **70**, 212409 (2004)
[28] A. Schnegg et al. Phys. Chem. Chem. Phys. **11**, 6820 (2009)
[29] J. Stöhr, H. C. Siegmann, *Magnetism* Solid-State Sciences **152** Springer, Berlin (2006)